Applied Thermal Engineering 221 (2023) 119928

Contents lists available at ScienceDirect

Applied Thermal Engineering

journal homepage: www.elsevier.com/locate/apthermeng

Integration of a heating and cooling system driven by solar thermal energy and biomass for a greenhouse in Mediterranean climates

J. Prieto [a,*], R.M. Ajnannadhif [a], P. Fernández-del Olmo [b], A. Coronas [a]

[a] Universitat Rovira i Virgili, Mechanical Engineering Department, CREVER. Avda. Països Catalans 26, 43007 Tarragona, Spain

[b] Andalusian Institute for Research and Training in Agriculture and Fisheries, Food & Environment (IFAPA), Camino San Nicolás n° 1, 04745 La Mojonera, Almería, Spain

ARTICLE INFO

Keywords:
Solar heating and cooling
Biomass
Greenhouse
Environmental control

ABSTRACT

World population growth, climate change, and water scarcity will increase food vulnerability, especially in developed countries. Therefore, increasing crop productivity is one of the main challenges to be addressed in the next years. In this sense, intensive horticulture will play a key role to supply the growing demand for food. In greenhouse farming in Mediterranean climates the passive control of the greenhouse ambient conditions is insufficient and, therefore, the use of active heating/cooling systems is required.

The status of solar thermal, biomass, and absorption heat pump technologies makes the active management of greenhouse climate conditions technically feasible. At the same time, the utilization of solar thermal and biomass energies allows reducing, as much as possible, the consumption of natural resources and the generation of waste.

In this study, we present a system based on solar thermal energy, biomass, and an air-cooled absorption chiller that are integrated to control the temperature of a greenhouse for tomato production in Mediterranean climates. The greenhouse thermal demand is firstly modelled with the TRNBuild tool and validated with real data obtained from a monitored greenhouse in southern Spain. The validated model is used to both study the system operation and determines the annual heating and cooling demands of a greenhouse with tomato crop (26.31 $kW{\cdot}h{\cdot}m^{-2}$, and 61.97 $kW{\cdot}h{\cdot}m^{-2}$, respectively), the energy performance of the system (solar fraction 54.92 %, and absorption chiller seasonal COP 0.624), and the annual biomass operational cost (2.70 $€{\cdot}m^{-2}$). This study also provides the specification of the main components (absorption chiller capacity, solar collector technology, absorbance area, biomass boiler thermal capacity, and water tank volume…) that can achieve these results. Moreover, the control for different typical days is shown.

1. Introduction/background

Food vulnerability is one of the main challenges to be addressed in the following years as the world population is expected to keep on increasing, and climate change and water scarcity will make the current crops decrease their productivity [1]. In this sense, intensive horticulture will play a key role to supply the growing demand for food with high productivity about other conventional crops.

Currently, competitiveness is one of the main problems in the horticultural sector in European Mediterranean areas due to the liberalization of the market. This issue forces the development of production systems that guarantee high productivity and quality. In addition, the current challenge of this sector is to achieve environmentally sustainable food security (availability, access, stability, and use) in a world of low emissions. In this formula, intensive horticulture plays a fundamental role in contributing to supplying the growing demand for food with high efficiency concerning other production systems.

Moreover, Mediterranean climate conditions are obstacles to all-year-round cultivation. Passive greenhouses, which rely only on natural ventilation and shading to cool the greenhouse, can only guarantee an appropriate internal microclimate whenever the outside temperature and humidity conditions are within the biological range that enables successful growth and production (12 to 29 °C temperature and 50 to 90 % relative humidity [2]) for most greenhouse typically cultivated species. In hot and warm regions, this may only happen during limited periods of the year. Thus, a cooling system, which can decrease the greenhouse temperature while maintaining humidity values within the optimum range, is essential to secure year-round quality food production.

* Corresponding author.
E-mail address: juan.prieto@urv.cat (J. Prieto).

https://doi.org/10.1016/j.applthermaleng.2022.119928
Received 15 February 2022; Received in revised form 2 December 2022; Accepted 19 December 2022
Available online 21 December 2022

Nomenclature

a_0	Solar collector intercept efficiency (-)
a_1	Solar collector slope efficiency ($W \cdot m^{-2} \cdot K^{-1}$)
a_2	Solar collector curvature efficiency ($W \cdot m^{-2} \cdot K^{-2}$)
A	Area (m^2)
c	Thermal capacity ($kJ \cdot kg^{-1} \cdot K^{-1}$)
C_{dT}	Discharge coefficient (-)
C_w	Wind effect coefficient (-)
COP	Coefficient of performance (-)
G_0	Solar radiation (kW)
g_E	Transpiration conductance ($m \cdot s^{-1}$)
h	Specific enthalpy ($kJ \cdot kg^{-1}$)
$K(\theta)$	Incidence angle modifier (-)
M	Volume flow rate ($m^3 \cdot s^{-1}$)
ms_v	Enclosure infiltration rat ($m^3 \cdot s^{-1}$)
RH	Relative humidity (%)
Q	Thermal energy (kW·h)
$\dot{Q}$	Heating or cooling rate (kW)
SF	Solar Fraction (-)
T	Temperature (°C)
U	Envelopment heat transfer coefficient ($kW \cdot m^{-2} \cdot K^{-1}$)
v_{air}	Wind speed ($m \cdot s^{-1}$)
w	Humidity ratio ($kg_w \cdot kg_{da}^{-1}$)

Greeks

λ	Latent heat of water vaporization ($kJ \cdot kg^{-1}$)
ρ	Density ($kg \cdot m^{-3}$)
τ	Enclosure g-value (-)
θ	Incidence angle (°)
η	Efficiency (-)

Subscripts

amb	Ambient conditions
av	Average
boil	Boiler
calc	Calculated
env	Envelopment
ev	Evaporator
gen	Generator
GH	Greenhouse
Heat	Heating
in	Indoor conditions
inf	Infiltration
L	Longitudinal
lat	Latent heat
max	Maximum
meas	Measured
min	Minimum
month	Monthly
s	Soil ground
SC	Solar collector
sen	Sensible heat
SS	Solar system
Set	Set point temperature
sun	Sun
T	Transversal
trans	Transpiration
vent	Ventilation

Essentially, there are two main approaches to cool greenhouses, evaporative and mechanical cooling. With these two approaches, the grower must use either a high amount of water and a reasonable amount of electricity (evaporative cooling) or close the greenhouse and use very little water but high amounts of electricity (mechanical cooling). Evaporative cooling systems are widely extended in arid regions with very dry ambient conditions. The most common technologies of this type are pad and fan systems, and to a lesser extent, fogging systems. With these technologies, the drier the ambient, the higher the cooling capacity that can be achieved. This means that, in most cases, it is possible to ensure that the crop remains within an optimum range of temperature and humidity ([3,4]). However, this is obtained at the expense of using very large amounts of water. Fuchs et al. [5] demonstrated that the amount of water consumed in such systems easily exceeds the water used for irrigation, whenever ambient relative humidity is lower than about 50 %. Sabeh et al. [6] reported 4 times higher water consumption for (evaporative) cooling than for tomato crop irrigation. In addition, pad and fan cooled greenhouses usually have undesired longitudinal microclimate gradients, and maintenance of the pads is time-consuming if water quality is low. Finally, in many coastal regions, which experience high ambient humidity values, evaporative cooling is simply not an option due to its lower cooling effect.

The other typical alternative is to close the greenhouse and use active/mechanical cooling to remove the excess sensible and latent heat from the greenhouse. This option has many advantages from the cultivation and sustainability perspective: it can save an enormous amount of water since all transpiration can be recovered by condensation in the coolers, it also allows for high CO2 values that will increase the yield, and it minimizes the entrance of pests and diseases, limiting the number of chemicals that need to be used to control them. There are very little data published on the performance of closed greenhouses in Mediterranean areas. Zaragoza et al. [7] measured recovery of up to 80 % of the total irrigation water by lixiviation and condensation (further reused in irrigation), and the added collection of rainfall in the Watergy prototype. However, the potential for larger yields was not fully exploited since the climatic conditions were not optimized for fruit production. In this sense, there are some interesting results obtained in the ESTIDAMAH research complex in Riyadh (Saudi Arabia) [8], in which yield increases of 50 % for tomatoes obtained in a closed greenhouse concerning the greenhouses with evaporative cooling with a water-saving factor 20 per kg of product. However, this achievement was obtained at the expense of using as much as 600 $kWh \cdot m^{-2} \cdot year^{-1}$ in electricity for cooling the greenhouse.

The status of solar thermal, biomass, and, especially, absorption heat pump technologies make, nowadays, technically feasible the active management of the greenhouse climate conditions for both heating and cooling production ([9,10]). In this sense, absorption heat pumps have been scarcely used for greenhouse applications mainly due to the system complexity and the requirement of cooling towers. Thus, only a few research papers are found in the literature in this regard. Campiatti et al. [11] evaluated a solar cooling system with a water/LiBr absorption chiller in Italy, concluding that very high energy savings can be achieved with this configuration.

At the same time, the utilization of solar thermal and biomass energies allows reducing, as much as possible both, the consumption of natural resources, and the generation of waste permitting, at the same time, the heating and cooling system is completely autonomous. In this sense, a combination of both technologies may contribute to finding a cost-effective and environmentally friendly method to increase crop productivity in Mediterranean climates.

In this sense, the combination of the three technologies together for a greenhouse located in Mediterranean climates has not been studied yet. Especially, considering the use of the air-cooled absorption chiller, and the biomass boiler. The combination of these technologies may autonomously provide environmental control and CO_2 enrichment, which increases crop productivity, with low environmental impact, and with low water requirements.

On the other hand, dynamic simulations are highly recommended to analyze the seasonal performance of heating and cooling systems, especially when solar energy takes place, as the available and the required energy changes with time and environmental conditions have a huge impact on the system's performance. Several studies have used dynamic simulation tools to get the seasonal performance and the energy demand in different kinds of greenhouses. Shamim et al. [12] modelled the thermal demands of a greenhouse in China using solar energy with dynamic simulation. Vadiee and Martin [13] modelled through dynamic simulation the potential of using excess heat from the greenhouse with thermal energy storage technology. Zhang et al. [14] studied the feasibility of seasonal thermal energy storage to heat a 231 m^2 tunnel greenhouse in Shanghai, China. Agrebi et al. modelled a solar-assisted water-to-water heat pump for heating a greenhouse in Tunisia [15].

The main objective of this study is to analyze the seasonal performance of a heating and cooling system, with solar thermal collectors, a biomass boiler, and an air-cooled absorption chiller, for the environmental control of a greenhouse in Mediterranean climates. The seasonal performance is analyzed in terms of indoor air conditions achieved by the system, heating, and cooling demands, heating and cooling peak loads, solar and biomass energy production, absorption chiller energy production and seasonal COP, solar fraction, and biomass cost. To achieve this, a dynamic model of the thermal loads of the greenhouse is first developed with TRNBuild. This model is validated with measured data from a greenhouse placed in La Mojonera (Almería), Spain. The proposed heating and cooling system is modelled in TRNSYS to obtain the seasonal performance and analyze the system operation under different representative days of the year for winter and summer conditions. The model and results of this study will be used as a starting point for other studies that will allow us to carry out a detailed economic study as both indoor air conditions and energy requirements can be calculated. Thus, the economic feasibility will be studied, considering the investment costs, the maintenance and operational costs, the required space, the crop production, and the product prices.

2. Methodology

The methodology section contains a description of the studied greenhouse. Then, it is briefly described the developed greenhouse thermal model, paying special attention to the transpiration and ventilation thermal loads. After that, the proposed heating and cooling system is presented, including the layout and the operating conditions for summer and winter days. Together with the heating and cooling system presentation, the main components of the system are detailed. Finally, a summary of the ambient conditions is presented.

2.1. Greenhouse description

The studied greenhouse is located in the Andalusian Institute for Research and Training in Agriculture and Fisheries, Food & Environment (IFAPA), Center "La Mojonera" (Almería, Spain, latitude 36° 30' N, longitude 2° 18' W). The main characteristics of this greenhouse are detailed in Table 1.

Fig. 1 shows a picture of the mentioned greenhouse. This greenhouse is currently equipped with a heating system with flat plate solar thermal collectors and a biomass boiler fueled with olive pits. The heating system only operates for the cooler days of the year. In addition, in the exhaust of the boiler, there is a CO_2 capturer based on activated carbon [16]. The captured CO_2 is supplied into the greenhouse to enhance crop productivity through an enrichment CO_2 system. Moreover, the greenhouse is equipped with a piped water heating system and a mobile shading screen. It also contains a complete monitoring system for the measurement of solar radiation, wind speed and direction, ambient temperature and relative humidity, and inside CO_2 levels, temperature, and relative humidity sensors [17].

Table 1
Main characteristics of the greenhouse.

Characteristic	Value	Description
Type of greenhouse	–	Gabled plastic roof
Kind of crop	–	Tomato
Orientation	10°	NW
Number of spans	4	–
Roof slope	38°	–
Height to the ridge (m)	7.2	–
Height to the gutter (m)	5.0	–
Length (m)	50.0	–
Width (m)	22.4	–
Greenhouse area (m^2)	1120.0	–
Side vents (opening area m^2)	240.0	In NW and SE facades, windows with opening control
Enclosure thermal conductivity ($W \cdot m^{-2} \cdot K^{-1}$)	8.0	Enclosure material is PEBD
Enclosure g-value (%)	90.0	Enclosure material is PEBD

2.2. Greenhouse thermal model description

To obtain the heating and cooling demands and the internal moist air conditions, the Type56b with the TRNBuild tool of TRNSYS has been used [18]. This tool is specially conceived for the modelling of multizone buildings in which each zone is a non-geometrical balance model with one air node per zone, representing the thermal capacity of the zone air volume and capacities, which are closely connected with the air node. The main reason for using this component of TRNSYS is that it can be easily coupled with the heating and cooling system. However, as this component is mainly thought for the heating and cooling demands of a conventional building, special attention must be paid when modelling crop transpiration and natural ventilation.

Fig. 2 shows the main thermal loads involved in the greenhouse energy balance. These are the radiative gains from the sun (τG_0), the radiative losses with the sky ($\dot{Q}_{sky}$), the heat transfer with the environment through the envelopment ($\dot{Q}_{env}$) (this accounts for both the heat conduction and the heat convection), the heat transfer with the soil ground ($\dot{Q}_s$), the heat gains/losses due to the natural ventilation (this accounts for both infiltration and ventilation through windows, $\dot{Q}_{inf}$ and $\dot{Q}_w$), and the internal gains due to the crop transpiration ($\dot{Q}_{trans}$). Apart from crop transpiration, other internal gains such as lightning, equipment, and people have been neglected. In particular for lightning, according to Valera et al. [19] who surveyed the technologies implemented in greenhouses located in the Almeria region, from all the greenhouses that participated in this survey, none of them contained lightning. This is due to the high number of sunlight days in Almería, which makes unprofitable their use.

More details about the TRNSYS TRNBuild tool can be found in [18]. For this particular application, according to Fig. 2, and from the overall energy and mass balances. The rate of change of internal energy for the greenhouse is equal to the net heat gain or:

$$c_{GH} \bullet \frac{dT_{in}}{dt} = \left(\dot{Q}_{sun} + \dot{Q}_{env} + \dot{Q}_{sen,inf} + \dot{Q}_{sen,w} - \dot{Q}_s - \dot{Q}_{sky}\right) \quad (1)$$

where c_{GH} is the thermal capacitance of the greenhouse.

The rate of change of moisture content on the greenhouse is equal to the latent energy ratios over the latent heat of water vaporization (λ) latent heat of water vaporization or:

$$\frac{dw_{in}}{dt} = \frac{1}{\lambda} \bullet \left(\dot{Q}_{trans} + \dot{Q}_{lat,inf} + \dot{Q}_{lat,w}\right) \quad (2)$$

Fig. 1. Greenhouse at the center of IFAPA “La Mojonera”.

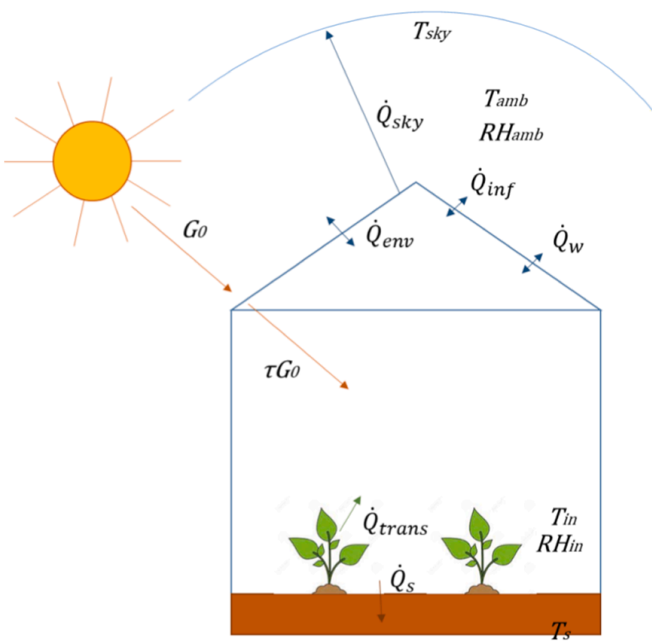

Fig. 2. Main thermal loads involved in the greenhouse energy balance.

The heat gains due to the sun ($\dot{Q}_{sun}$) only considers the radiative part of the non-opaque surfaces. The model splits the external solar radiation into a visual part and a non-visual part. The model calculates then for the visual and for the non-visual part separately the reflection, the absorption on single panes and the distribution within the greenhouse including multiple reflection. The absorbed and transmitted radiation is summed up to get the total solar absorbed or transmitted radiation. More details can be found in [18].

The heat transfer with the environment through the envelopment ($\dot{Q}_{env}$) accounts for the conduction and the convection heat transfer rates. The heat flux for every single surface ($\dot{Q}_{env,i}$) is calculated as:

$$\dot{Q}_{env,i} = U_i \bullet A_i \bullet (T_{amb} - T_{in}) \quad (3)$$

The heat losses to the ground ($\dot{Q}_s$) accounts for the conduction and the convection heat transfer rates. The ground temperature has been set as a boundary condition that changes with time following the equation provided by Kasuda and Archenback [20], which depends on the mean annual ambient temperature, the depth below the surface, and the soil thermal conductivity, density, and heat capacity.

The radiative heat losses to the sky ($\dot{Q}_{sky}$) are also considered in the model as a long-wave radiation. More details are described in [18].

As it is previously mentioned, special attention must be paid when modelling the crop transpiration and the natural ventilation. For the crop transpiration, the used model is based on the described by Stanghellini and Jong [21], which is calculated as:

$$\dot{Q}_{trans} = g_E \bullet \lambda \bullet \left(w_{crop} - w\right) \quad (4)$$

where, λ is the latent heat of vaporization of water, w_{crop} is the absolute water vapor concentration in the crop, w is the humidity ratio in the greenhouse, and g_E is the transpiration conductance, which depends on the latent and sensible heat in the saturated air, the solar radiation, and the ambient temperature. The detailed model to calculate g_E can be found in [22].

The heat gains due to the natural ventilation ($\dot{Q}_{vent}$), this is infiltration and natural ventilation through windows, the air volumetric flow rate, M_{vent}, entering the greenhouse is calculated with the equation given by Ruiz-García et al. [23]:

$$\dot{Q}_{vent} = \dot{Q}_{inf} + \dot{Q}_w \quad (5)$$

$$\dot{Q}_{vent} = M_{vent} \bullet \rho_{amb} \bullet (h_{env} - h_{in}) \quad (6)$$

$$M_{vent} = \left(\frac{A_{wind}}{2}\right) \bullet C_{dT} \bullet \sqrt{C_w} \bullet v_{air} + ms_v \quad (7)$$

where, A_{wind} is the window area, C_{dT} is the discharge coefficient that depends on the windows geometry, C_w is the wind effect coefficient, v_{air} is the wind speed, and ms_v is the infiltration rate that depends on the enclosure area. More details about the natural ventilation calculation are found in [22]. Table 2 contains the main parameters used for the greenhouse thermal model.

2.3. Proposed heating and cooling system description

The proposed configuration for the greenhouse environmental control is shown in Fig. 3. As can be seen from this Figure the main

Table 2
Main parameters for the greenhouse thermal model.

Parameter	Value
Thermal capacitance of the greenhouse (kJ/K)	30,000
Enclosure thermal conductance (W·m^{-2}·°C^{-1})	8.0
Enclosure g-value (%)	90.0
Window area (m^2)	240.0
Discharge coefficient (-)	2.21
Wind effect coefficient (-)	0.14
Infiltration rate (m·s^{-1})	9.36
Soil density (kg·m^{-3})	3,200
Soil thermal conductivity (W·m^{-1}·°C^{-1})	2.42
Leaf area index (-)	2.2
Boundary layer resistance parameter (-)	200

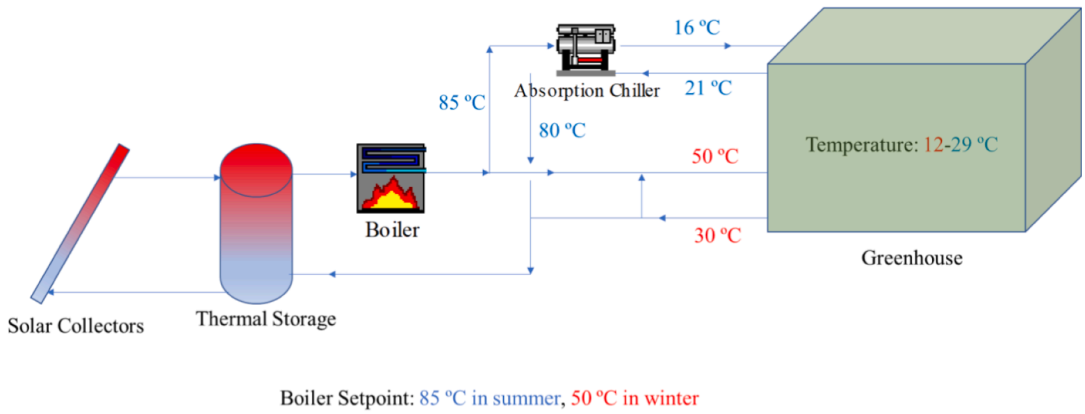

Fig. 3. Solar thermal and biomass system for the greenhouse environmental control.

components are the solar collectors, the thermal storage, the biomass boiler, and the air-cooled absorption chiller. Despite this heating and cooling system is well known in other applications, greenhouses have not been studied in detail before, mainly due to the complexity of the system and the requirement of a cooling tower for most of the absorption chillers, which leads to higher investment and maintenance costs as well as greater space requirements and water for the cooling tower operation. However, this configuration presents some benefits:

- The system allows producing heating or cooling, depending on the greenhouse requirements. Therefore, the greenhouse can be in operation for the complete year, which increases its productivity, especially in Mediterranean areas, where heating is required in winter and cooling in summer.
- By combining solar energy and biomass, the system is completely autonomous, especially if organic waste from the crop is used to operate the biomass boiler. In addition, CO_2 from biomass combustion can be trapped and injected into the greenhouse to increase crop productivity.
- The proposed absorption chiller uses ammonia-lithium nitrate as working pair. Due to its low crystallization risk, this mixture allows an air-cooled heat rejection, and therefore, a cooling tower is not required, which simplifies the system, reduces the investment and maintenance costs, and the required space in comparison with water-lithium bromide-based absorption chillers.

The ammonia-lithium nitrate absorption chiller technology is not available in the market yet. However, this technology has studied and demonstrated for years [25]. With respect the technologies currently available in the market, water-lithium bromide and ammonia-water, it can be air-cooled (water-lithium bromide chillers need cooling tower), and it does not require a rectifier (ammonia-water chillers need rectifier). Therefore, this technology is more suitable for applications where space and maintenance are important.

As the temperature level for the absorption chiller activation is 85 °C, it is proposed to replace the flat-plate solar collectors currently installed in the greenhouse with evacuated-tube solar thermal collectors due to their higher efficiency at this temperature level. This technology of solar thermal collectors is available in the market for years.

In case the evacuated-tube solar thermal collectors do not provide enough heat for the greenhouse or the absorption chiller, a biomass boiler operates to handle the heating required. This biomass boiler uses olive pits as fuel. As heating is required at 50 °C and the activation temperature of the absorption chiller is 85 °C, the set point temperature of the boiler is changing throughout the year. This is not a technical problem as heating is only required by the greenhouse during the winter months and cooling during the summer months. This boiler technology is available also in the market, as the solar thermal collectors.

To increase crop productivity, temperature control is very important, especially for tomatoes. For this vegetable, bad temperature control increases the risk of illness and reduces the quality of the product. In this sense, the highest productivity and quality of tomatoes is reached when the air temperatures are kept between 29 °C and 12 °C [2]. The maximum allowed relative humidity is 80 %. Therefore, heating will be required to handle the minimum crop temperature, which is 12 °C, and cooling will be required to handle the maximum crop temperature, which is 29 °C. With these air temperatures required, the heating and cooling system can operate at suitable temperatures to maximize its performance; this means that the design temperature for the cooling production is 16/21 °C and the design temperature for the heating production is 50/30 °C. For the absorption chiller, the design temperature for the generator is 85 °C.

2.4. Heating and cooling system model description

This system is modelled on TRNSYS and coupled to the greenhouse thermal model to obtain the seasonal performance of the heating and cooling system and the indoor air conditions reached with it.

The air-cooled absorption chiller is modelled with the characteristic equation developed by Hellman et al. [24]. This model can obtain both the cooling capacity and the heating required of single-effect absorption chillers using simple algebraic equations. These equations are expressed as a function of the so-called characteristic temperature difference, which depends on the average temperature of the external circuits, and a parameter representing the slope of an average solution isothere in the Dühring chart. Equations (5) and (6) show the "*characteristic equation*" set [25] for the cooling capacity, $\dot{Q}_{ev}$, and the heating required, $\dot{Q}_{gen}$ by the proposed absorption chiller:

$$\dot{Q}_{ev} = -12.3323 \bullet T_{amb} + 7.6740 \bullet T_{ev} + 4.9100 \bullet T_{gen} + 56.6522 \tag{8}$$

$$\dot{Q}_{gen} = -17.7478 \bullet T_{amb} + 9.9620 \bullet T_{ev} + 8.3931 \bullet T_{gen} + 24.4464 \tag{9}$$

The corresponding thermal coefficient of performance (*COP*) is calculated as the ratio of cooling capacity to heating required, this is:

$$COP = \frac{\dot{Q}_{ev}}{\dot{Q}_{gen}} \tag{10}$$

Fig. 4 shows the graphical representation of the absorption chiller cooling capacity and *COP* as a function of the ambient temperature and the inlet hot water temperature when the chilled water set point temperature (T_{set}) is 16 °C (see Fig. 5).

As it is mentioned above, it is proposed to replace the flat-plate solar thermal collectors by the evacuated-tube type. Solar thermal collectors are modelled with the efficiency method, considering that the incidence angle modifier changes with longitudinal and transversal angles. In this

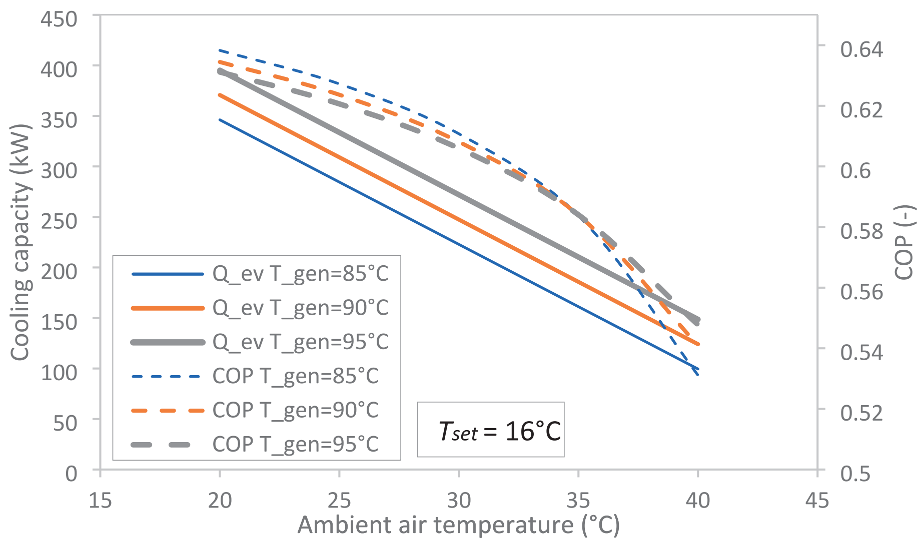

Fig. 4. Absorption chiller cooling capacity and COP as a function of the ambient temperature and the inlet hot water temperature.

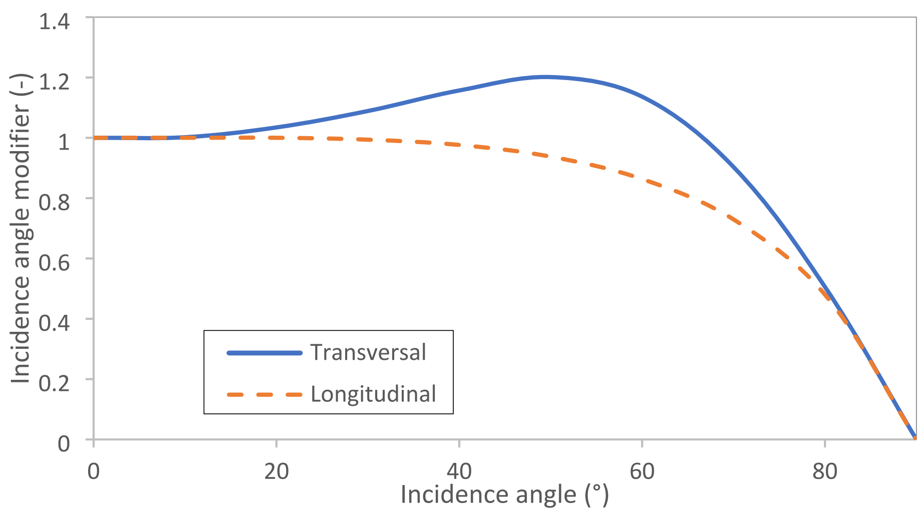

Fig. 5. Solar thermal collector longitudinal and transversal incidence modifiers [25].

sense, the thermal efficiency of the solar collectors is calculated with the following empirical equation:

$$\eta_{SC} = \frac{\dot{Q}_{SC}}{G_0} = a_0 \bullet K(\theta) - a_1 \bullet \frac{(T_{av} - T_{amb})}{G_0} - a_2 \bullet \frac{(T_{av} - T_{amb})^2}{G_0} \tag{11}$$

where $\dot{Q}_{SC}$ is the fluid heating rate in the solar collectors, G_0 is the total solar irradiance, T_{av} is the average temperature of the solar collectors, T_{amb} is the ambient temperature, θ is the incidence angle, a_0, a_1, a_2 are the efficiency parameters, and $K(\theta)$ is the incident angle modifier, which are empirical values provided by the manufacturer. The incident angle modifier is calculated as the product of a transversal (K_T) and a longitudinal (K_L) function:

$$K(\theta) = K_T(\theta_L = 0; \theta_T) \bullet K_L(\theta_L; \theta_T = 0) \tag{12}$$

For this case, the empirical values used are shown in Table 3.

On the other hand, the nominal thermal efficiency of the biomass boiler is 0.861, this efficiency is remained constant for the whole year. The water tank has a volume of 20 m^3 which represents a water-storage volume to solar-collector area ratio of about 100 $l_{water} \cdot m_{SC}^{-2}$. Table 4 summarizes the main specifications of the system components.

Table 3
Technical characteristics of solar thermal collectors [26].

Parameter	Value	Description
Dimensions (mm)	1895, 624, 75	Length, width, height
Absorber area (m^2)	0.95	–
Reflector area (m^2)	1.05	–
Total collector area (m^2)	1.18	–
Number of tubes (-)	6	–
Concentration (-)	1.08	–
a_0 (-)	0.781	Based on the absorber area
$a_1 \left(\frac{W}{m^2 \bullet K}\right)$	1.985	Based on the absorber area
$a_2 \left(\frac{W}{m^2 \bullet 8K^2}\right)$	0.004	Based on the absorber area
Long. incidence angle modifier (50°)	0.93	–
Trans. Incidence angle modifier (50°)	1.20	–
Volume Flow rate ($l \cdot h^{-1}$)	10–500	–
Max. operating pressure (bar)	10	–
Max. recommended operating temperature (°C)	160	–

Table 4
Main specifications of the system components.

Component	Parameter	*Value*
Solar thermal collectors	Absorption area (m^2)	200.6
Water tank	Volume (m^3)	20.0
	Height (m)	4.67
	Tank loss coefficient ($W \cdot m^{-2} \cdot K^{-1}$)	0.02
Boiler[(a)]	Heating capacity (kW)	350.0
	Nominal efficiency (-)	0.861
	Minimum operation temperature (°C)	50.0
	Maximum operation temperature (°C)	95.0
Absorption chiller[(b)]	Nominal cooling capacity (kW)	220.0
	Nominal COP (-)	0.61

[(a)] Nominal conditions for the boiler are considered following the UNE EN 303–5-1999 standards.
[(b)] Nominal conditions for the absorption chiller are considered at full load with an ambient air temperature of 30 °C, an activation temperature of 85 °C, and a chilled water temperature of 16 °C.

2.5. Ambient conditions

To have an overview of the weather conditions of the studied location, Fig. 6 (a) and (b) shows the monthly mean, the maximum and the minimum ambient dry bulb temperatures, the monthly total horizontal radiation, and the mean monthly humidity ratio for Almería. As can be observed, the ambient temperature is warm for six months (from May to October), with mean ambient temperatures in the range of 20 °C. Minimum temperatures are lower than 12 °C from November to April and maximum temperatures are higher than 29 °C from May to September. The solar radiation available in summer months (225 $kW \cdot h \cdot m^{-2}$) is almost three times the available in winter months (80 $kW \cdot h \cdot m^{-2}$). The annual total horizontal radiation in this location is 1,800 $kW \cdot h \cdot m^{-2}$. Weather data has been processed from the hourly data taken from the Energy Plus weather data for Almería, Spain [27].

3. Results and discussion

As it is mentioned in section 2.3, thanks to the combination of solar thermal collectors, with the biomass boiler and the air-cooled absorption chiller, the proposed system allows providing heating in winter, cooling and summer and CO_2 from biomass combustion. Thus, crop productivity is increased due to the controlled indoor air conditions and the CO_2 enrichment, with a system that is completely autonomous and simple, as cooling towers are not required. In this sense, compared with conventional heat pumps combined with photovoltaic panels, this system can provide CO_2 to the crop, it can store thermal energy in a cheaper way, and uses a natural refrigerant. On the other hand, compared with evaporative cooling systems, the proposed system can provide heating and CO_2, and requires less water.

The results and discussion section is divided into 5 subsections. The first one contains a comparison of the measured and the calculated indoor air conditions of the greenhouse to validate the thermal model developed. Once the model is validated, the heating and cooling demands of the greenhouse are presented. Then, it is included a detailed description of the system operation for the two typical days in both, winter, and summer conditions. After this description is done, the indoor air conditions of the greenhouse with and without a heating and cooling system are compared for the whole year. Finally, the seasonal performance of the proposed system is shown.

3.1. Greenhouse model validation

To validate the thermal model of the greenhouse, outputs calculated from simulations are compared with real measurements of the system during operation. The measured data is available with a time step of 15 min. The measured data used for this validation is the solar radiation, the ambient temperature, and relative humidity, the wind velocity and wind direction, the inside air temperature and relative humidity, the opening of the windows, and the operation of the heating system.

Table 5 shows the main specifications of the measuring devices used in the greenhouse, including the device type, the measurement accuracy, and the operational range.

The left-hand graph in Fig. 7 shows the comparison between the

Table 5
Specifications of the measuring devices.

Parameter	Device	Accuracy	Operational Range
Ambient dry-bulb temperature	4-wire Pt100	0.15 °C	−40–60 °C
Ambient relative humidity	Air relative humidity sensor	0.8 %	0–100 % RV
Ambient wind speed	Cup-rotating anemometer	0.5 ms^{-1} + 3 %	0–30 $m \cdot s^{-1}$
Ambient wind direction	Wind vane	2 %	0–359 °
Outside CO_2 concentration	CO_2 Transmitter Module	1.5 %	0–2000 ppm
Solar radiation	Pyranometer	1.5 %	0–1600 $W \cdot m^{-2}$
Greenhouse temperature	RTD [Pt100 (1/3DIN Class B)]	0.15 °C	−40–60 °C
Greenhouse relative humidity	Wet bulb sensor	2 %	5–95 %
Greenhouse CO_2 concentration	CO_2 Transmitter Module	1.5 %	0–2000 ppm

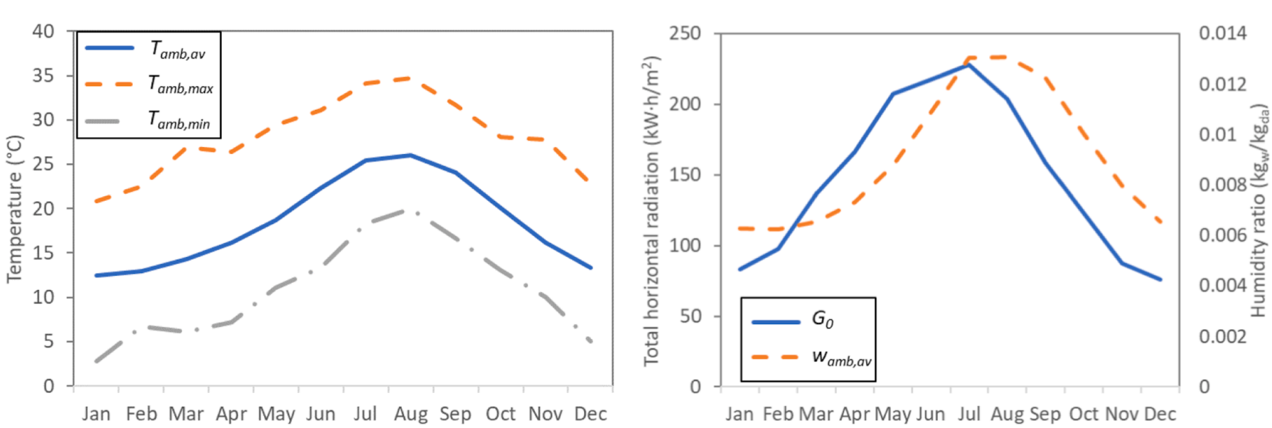

(a)

Fig. 6. Monthly mean ambient temperatures and humidity ratio values (a) and monthly total horizontal radiation (b) along the year [26].

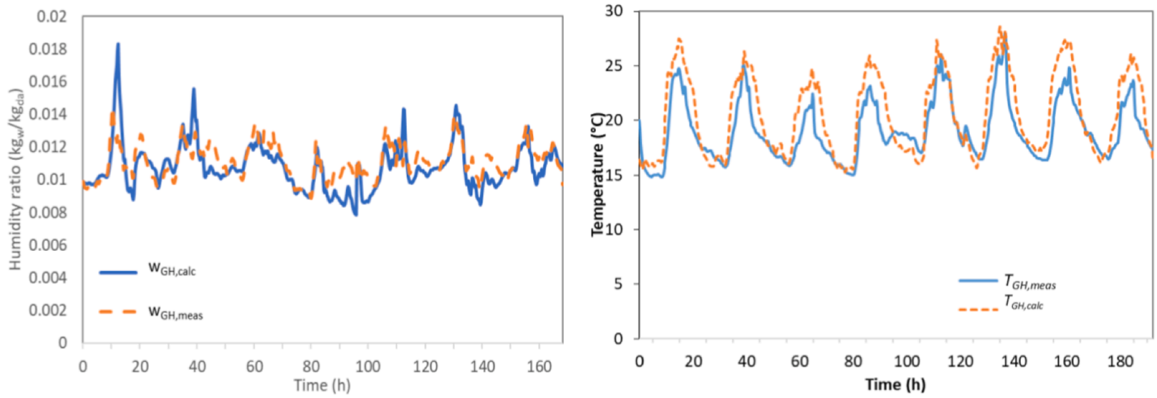

Fig. 7. Comparison between the calculated and measured greenhouse air humidity ratios (left) and between the calculated and measured greenhouse dry bulb temperatures (right) for a week in April.

inside air humidity ratios calculated from the dynamic simulation and the measurements of the real system for a week in April. Similarly, the right-hand graph in Fig. 7 shows the comparison between the greenhouse dry bulb temperatures calculated from the dynamic simulation and the measured values for the same week. According to the results, discrepancies between the calculated and measured humidity ratios and absorber water temperatures are very small.

Table 6 also shows a statistical comparison between the results obtained by the simulated model and the measured data during operation.

The mean discrepancies between the measured and the calculated data are 8.1 % for the humidity ratio, and 7.3 % for the air temperature. These discrepancies can be due to measurement uncertainties for the solar radiation, temperature, and relative humidity sensors. In summary, we can conclude that the model can be regarded as validated. Therefore, in the next sections, the model is used to calculate the heating and cooling demands and for the integration of the proposed system.

3.2. Heating and cooling demands

Once the thermal model of the greenhouse is validated, the annual heating and cooling demands can be obtained from it. Fig. 8 shows the monthly heating and cooling demands (sensible and latent) of the greenhouse. As can be observed from this Figure, heating is required from December to April, and cooling from April to October. In spring and autumn, the amount of heating/cooling required is very small.

The annual heating demand is 29,510 kW·h, and the annual cooling demand is 69,407 kW·h. This represents an annual energy ratio for heating of 26.37 kW·h·m^{-2} and 61.97 kW·h·m^{-2} for cooling.

Van't Ooster et al. [27] evaluated the heating and cooling demands of a semi-close greenhouse in Almería. In their case, the indoor air temperature was set at 16 °C and 26 °C in winter and summer respectively. Moreover, the cooling demands were not calculated during the months that the greenhouse is closed, this is July and August. Under these conditions, the heating and cooling demands calculated from the developed model are 138.04 kW·h·m^{-2} for heating and 51.61 kW·h·m^{-2} for cooling. The heating and cooling demands calculated by Van't Ooster et al. [28] are 172.22 kW·h·m^{-2} and 37.22 kW·h·m^{-2}, respectively. This represents a difference of 20 % and 28 % for heating and cooling demands respectively. These differences can be caused to a different control for the greenhouse ventilation and a different greenhouse cover, which consists of a single layer of plastic film and an internal shading screen combined with NIR whitewashing to control the solar radiation input.

Typically, the set point temperature for tomato crops is 27 °C. At this set point temperature, the annual cooling demand is 101,282 kW·h, which represents an annual energy ratio for cooling of 90.43 kW·h·m^{-2}, this is 45.9 % higher than the cooling demand when the set point temperature is 29 °C. This fact is due to two reasons: because cooling has to be applied for more hours of the year, and because the cooling rate has to be higher to keep the indoor air temperature at 27 °C. As the tomato crop can afford 29 °C with good productivity [2], and the greenhouse cooling demand is very affected by the temperature, it is decided to set 29 °C as a set point.

Table 6
Statistical comparison between measured and simulated data of some parameters of the system.

Statistical parameter	w_{in} ($kg_w \cdot kg_{da}^{-1}$)	T_{in} (°C)
Standard deviation	0.0009	1.5
Average calculated	0.01076	19.2
Average measured	0.01112	20.5

3.3. System operation

As the greenhouse requires heating during the winter months and cooling during the summer months, the proposed system needs to operate at very different working conditions throughout the year. Therefore, the system control must be able to satisfy these changing requirements efficiently. In this section, it is described the system's operation during two different working conditions, this is during typical winter days and during typical summer days.

Fig. 9 shows the system temperature evolution during two days of typical winter conditions. Temperatures represented in this graph are the water temperature at the top and the bottom of the tank, the boiler outlet-water temperature, the return water temperature from the greenhouse, and the greenhouse air temperature. As can be seen, during these days 5 different system operation modes (named modes A, B, C, D, and E) can be found. During conditions A, B, and C, the greenhouse temperature is at 12 °C, which means that the system must provide heating to the greenhouse to keep it at this temperature; during conditions D and E, the greenhouse temperature is higher than 12 °C, what means that no heating is required to be provided to the greenhouse. It is also interesting to observe that, during sunny hours, no heating is required by the greenhouse. Therefore, the hours when solar energy is available and the hours when the greenhouse requires heating are disengaged. Thus, the role of the water tank is especially important for the winter months.

Mode A occurs in the evenings and early at night. In this mode, heating is required and the water temperature at the top of the tank is higher than the required supply temperature (50 °C). During this period, the boiler and the solar circulation pump are off, the greenhouse circulation pump is off, and part of the return water is mixed with part of the water leaving the tank to provide the required supply water temperature. During this mode, all the heating required is provided by solar

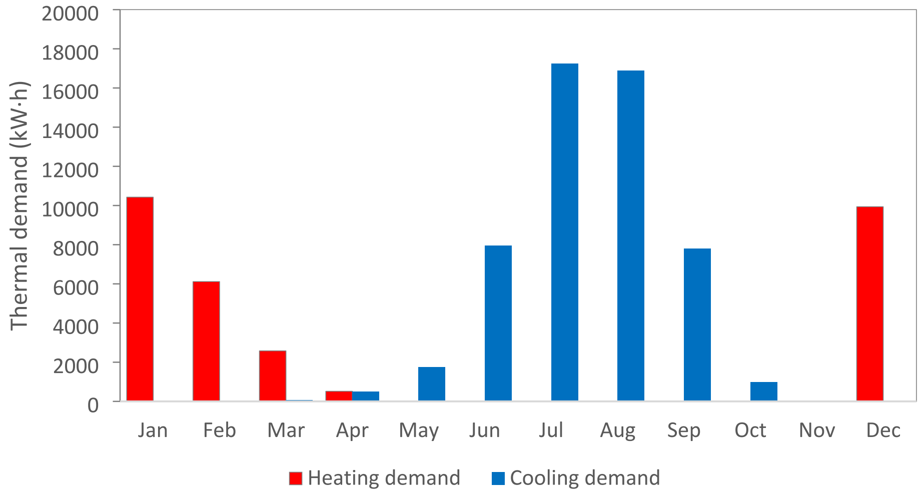

Fig. 8. Monthly thermal demands of the greenhouse throughout the year.

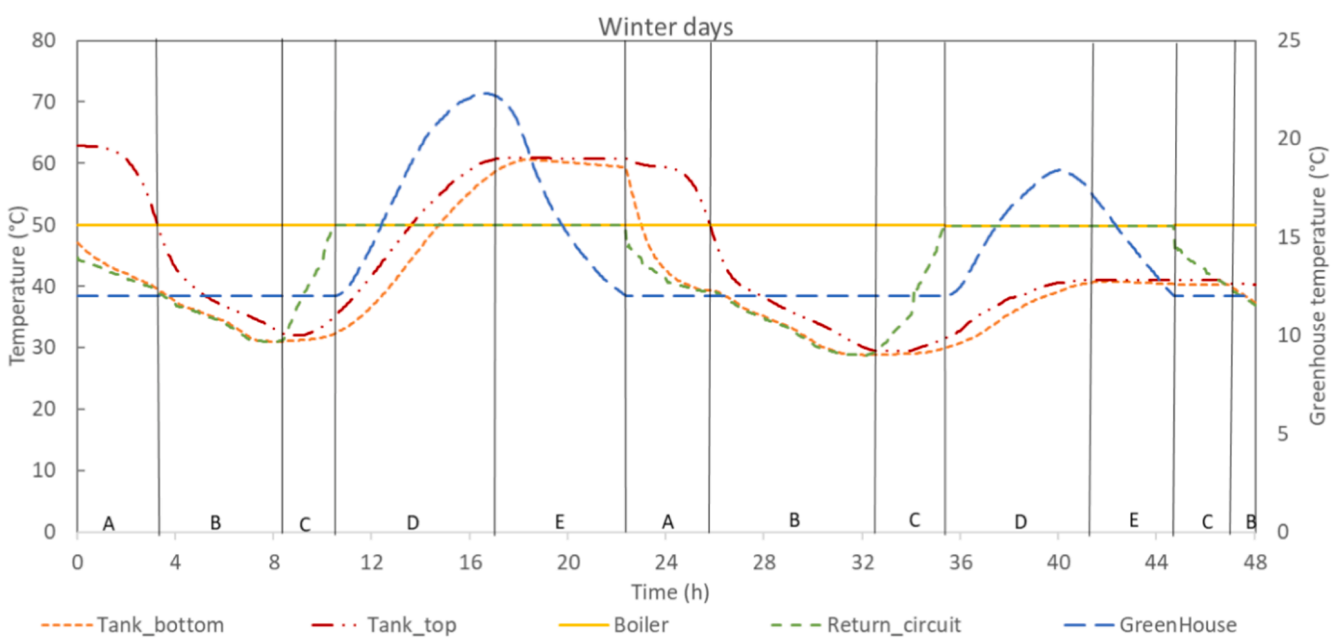

Fig. 9. System temperature evolution during two days of typical winter conditions.

energy previously stored. As this mode occurs when there is no solar radiation, the water temperature in the tank is decreasing with time.

Mode B occurs at night and at the beginning of the morning. In this mode, heating is required and the water temperature at the top of the tank is lower than the required supply temperature (50 °C) and higher than the return water temperature. During this period, the boiler and the greenhouse circulation pump are on, and the solar circulation pump is off. In this case, part of the heating is provided by solar energy previously stored and part by the boiler. As this mode occurs when there is no solar radiation, the water temperature in the tank is still decreasing with time.

Mode C occurs at the beginning of the morning. In this mode, less heating is required by the greenhouse. This means that the return water temperature is even higher than the water temperature at the top of the tank. Therefore, the boiler and the greenhouse circulation pump are on to heat the water, the solar circulation pump is off, and the return water of the greenhouse circuit is bypassing the tank to be directly provided to the boiler. During this period, all the heating is provided by the boiler. As this mode occurs when there is some solar radiation, the water temperature in the tank is starting to increase with time.

Mode D occurs during sunny hours. In this mode, no heating is required by the greenhouse and the water temperature at the top of the tank is increasing with time thanks to solar heating. During this period, both the boiler and the greenhouse circulation pump are off, and the solar circulation pump is on.

Mode E occurs after sunset. In this mode, no heating is required, and solar energy is not available. Thus, all the components of the system are off.

Fig. 10 shows the system temperature evolution during two days of typical summer conditions. Temperatures represented in this graph are the water temperature at the top and the bottom of the tank, the boiler outlet-water temperature, the return water temperature from the absorption chiller, the greenhouse air temperature, and the chilled water supply and return temperatures. As it can be seen, as in the case of the winter days, 5 different system operation modes (named mode A, B, C, D, and E) can be found. During conditions B, C, D, and E the greenhouse

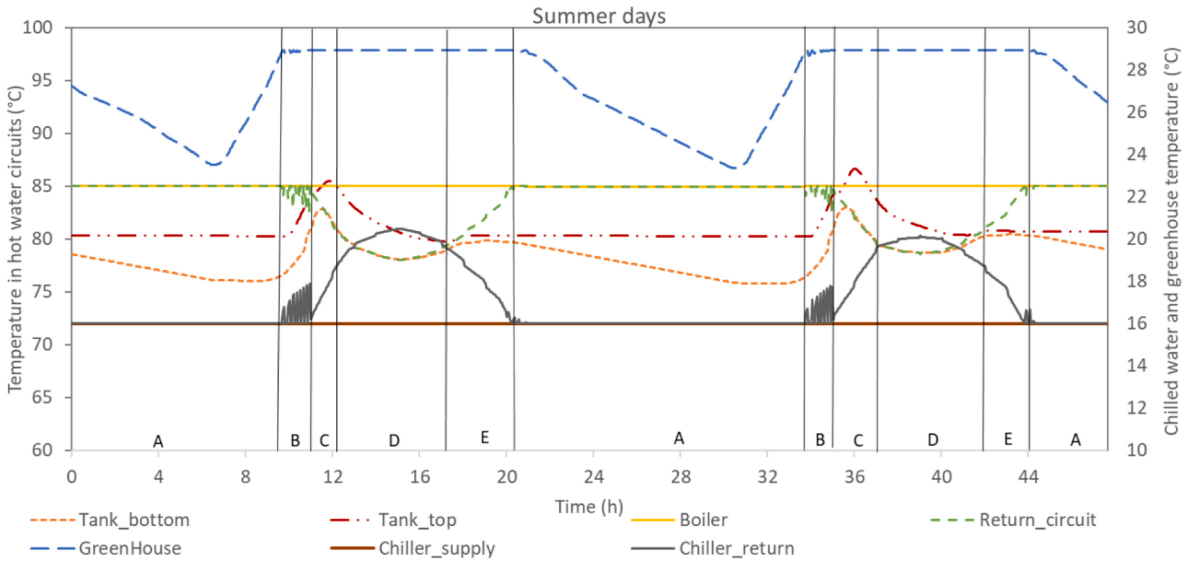

Fig. 10. System temperature evolution during two days of typical summer conditions.

temperature is at 29 °C, which means that the system must provide cooling to the greenhouse to keep it at this temperature. During conditions A, the greenhouse temperature is lower than 29 °C, which means that no cooling is required to be provided to the greenhouse. It is also interesting to observe that, during sunny hours, cooling is required by the greenhouse. Therefore, the hours when solar energy is available and the hours when the greenhouse requires cooling are almost engaged. Thus, the role of the water tank is not as important in the summer months as in the winter months.

Mode A occurs at night. In this mode, no cooling is required, and solar energy is not available. Thus, all the components of the system are off.

Mode B occurs at the beginning of the morning. In this mode, cooling is starting to be required. The water temperature at the top of the tank is lower than the return water temperature. At the same time, the water inside the tank is heated with solar energy. Therefore, the boiler and the solar circulation pump are on, the return water of the greenhouse circuit is bypassing the tank to be directly provided to the boiler, and the absorption chiller and the greenhouse circulation pump are controlled to keep the greenhouse temperature at 29 °C. As cooling loads are low in this period, the absorption chiller and the greenhouse circulation pump are starting and stop their operation following a hysteresis control. Due to this fact, fluctuations in the supply and return chiller water temperatures appear during this period. During Mode B, all the heating required by the absorption chiller is provided by the boiler. As this mode occurs when there is some solar radiation, the water temperature in the tank is starting to increase with time.

Mode C occurs in the midday. In this mode, heating is required to drive the absorption chiller and the water temperature at the top of the tank is higher than the required temperature to drive the absorption chiller (85 °C). Thus, during this period, the boiler is off, the absorption chiller and the greenhouse circulation pumps are on, and the solar circulation pump is also on. During this period, part of all the heating to drive the absorption chiller is provided by solar energy.

Mode D occurs in the afternoons when the greenhouse cooling demand is high. In this mode, the heating required to drive the absorption chiller is high and the water temperature at the top of the tank is lower than the required supply temperature (85 °C) and higher than the return water temperature. During this period, all the components of the system are on any part of the heating to drive the absorption chiller is provided by solar energy and part by the boiler. As the heating required by the absorption chiller is very high, the water temperature in the tank is decreasing with time.

Mode E occurs in the evenings. In this mode, the cooling required is lower. The water temperature at the top of the tank is lower than the return water temperature. At the same time, there is no solar radiation. Therefore, the boiler and the greenhouse circulation pump are on to heat the water, the absorption chiller is on, the solar circulation pump is off, and the return water of the greenhouse circuit is bypassing the tank to be directly provided to the boiler. During this period, all the heating to drive the absorption chiller is provided by the boiler.

3.4. Comparison with a passive greenhouse

As the main purpose of the heating and cooling system is to control the environmental conditions of the greenhouse, it is interesting to see how the indoor air conditions are over the year and compare them with the indoor conditions of a passive greenhouse. Fig. 11 (a) and (b) show the inlet air conditions of the greenhouse without a heating and cooling system (passive greenhouse) and with the proposed heating and cooling system (greenhouse with controlled temperature), respectively. Indoor air conditions are shown in terms of the daily average, maximum and minimum temperatures for the complete year. As can be observed in Fig. 11(b), the heating and cooling system can maintain the indoor air conditions at the required values for good crop productivity (this is represented with the blue space, and it corresponds to air temperature between 12 and 29 °C). This applies not only to the average daily temperature but also to the maximum and minimum temperatures, except for three days in the summer period when the maximum temperature exceeds 29 °C for a short period. In terms of daily average and minimum temperatures, they stay inside the required range of temperatures for the entire year.

On the other hand, as can be observed in Fig. 11 (a), the indoor air conditions of the passive greenhouse are extreme, especially the maximum air temperatures, which can reach values above 40 °C during the hottest days of the year. In addition, maximum air temperatures are above 29 °C for 33 % of the days of the year, especially from the beginning of May to the end of September. In terms of daily average values, indoor air temperature is above 29 °C from the beginning of July until the end of August. On the other hand, minimum air temperatures are below 12 °C for 27 % of the days of the year. Therefore, in passive greenhouses located in this region, during 60 % of the days of the year, indoor conditions are out of the required for good crop productivity, especially during summer months. For this reason, crop production is

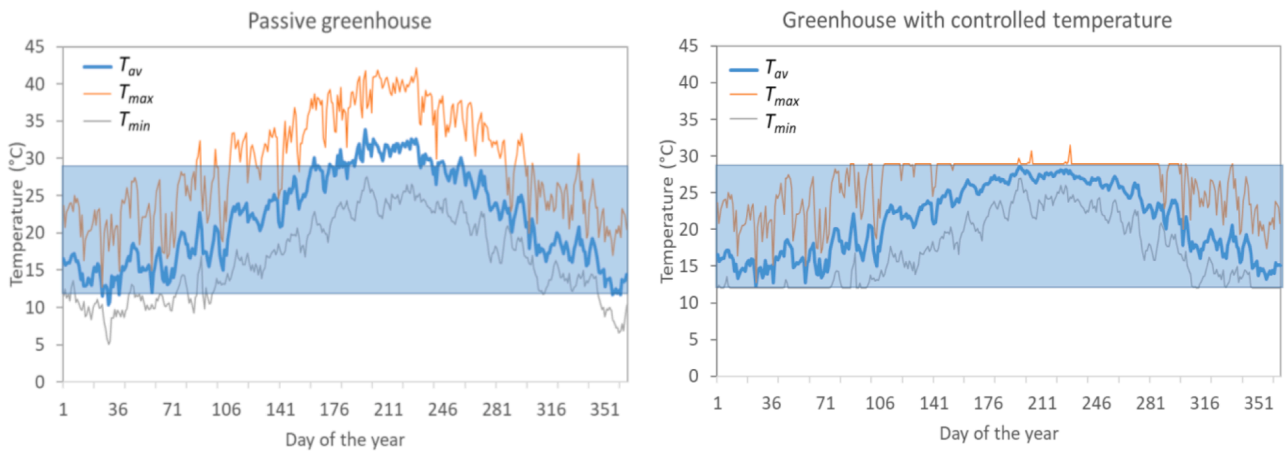

(a)

Fig. 11. Indoor air temperatures of a passive greenhouse (a) and a greenhouse with the proposed heating and cooling system (b) throughout the year.

usually stopped from the middle of May until the beginning of October, as the indoor air temperatures are too high.

Moreover, in the passive greenhouse, the relative humidity is 100 % for 49.3 % of the days, this especially happens during the coldest months of the year, this is from November to April. However, the relative humidity achieved with the greenhouse with controlled indoor conditions does not exceed 90 % for the whole year.

3.5. Seasonal performance of the integrated system

Once the system operation is analyzed and the greenhouse air conditions are met for the whole year, it is interesting to see the seasonal performance of the proposed heating and cooling system. Fig. 12 shows the monthly boiler consumption, solar thermal production and thermal energy required by the greenhouse (Q_{GH}). The thermal energy required by the greenhouse is the energy required to activate the absorption chiller and the heating required in the greenhouse. Therefore, it is calculated as:

$$Q_{GH} = \int \left(\dot{Q}_{gen} + \dot{Q}_{heat} \right) \bullet dt \tag{13}$$

As part of the thermal energy produced by the solar collectors is lost (e.g., the thermal losses in the water tank), the solar thermal production (Q_{SS}) is calculated as the difference between the total energy required (Q_{GH}) and the heating provided the boiler. Therefore, it is calculated as:

$$Q_{SS} = Q_{GH} - \int \dot{Q}_{boil} \bullet dt \tag{14}$$

As can be seen, the boiler only needs to work in the extreme months of the year, especially during the hottest months to activate the absorption chiller. This is especially important during July and August when the 61.4 % of the total boiler consumption takes place. On the other hand, during the spring and the autumn, the solar thermal production is higher than the thermal energy required to activate the absorption chiller and to heat the greenhouse. This fact is mainly due to the very small energy demands that the greenhouse has during these months. Therefore, the excess thermal energy could be used for other purposes or a more refined control of the greenhouse temperature, for instance, 18 °C for the minimum temperature and 25 °C for the maximum temperature. Moreover, the thermal energy required is higher than the solar thermal energy and the boiler consumption due to the boiler efficiency and the absorption chiller COP, which are lower than 1. This is especially relevant during the hottest months, whenthe absorption chiller is operating.

Fig. 13 (a) shows the monthly solar fraction (*SF*) of the proposed system. The solar fraction is defined as the solar thermal production (Q_{SS}) with respect to the total thermal energy required by the greenhouse (Q_{GH}):

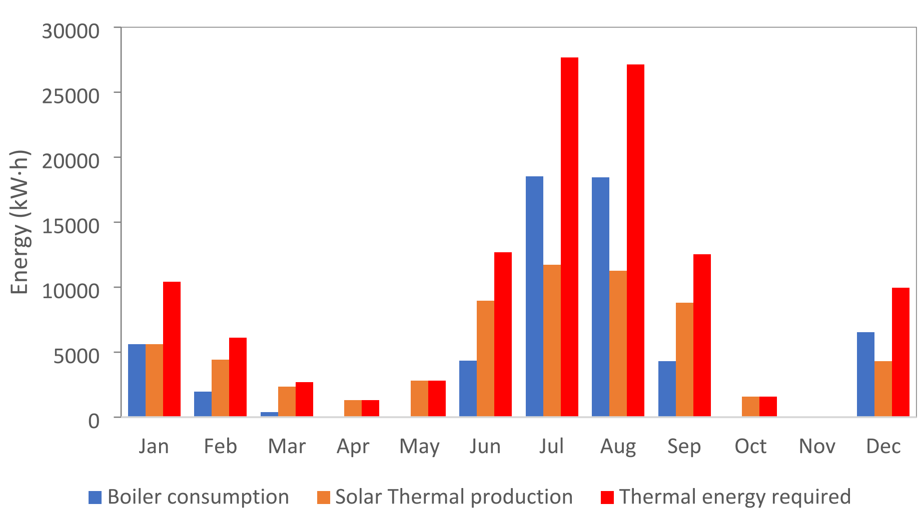

Fig. 12. Monthly boiler consumption, solar thermal production, and thermal energy required by the greenhouse.

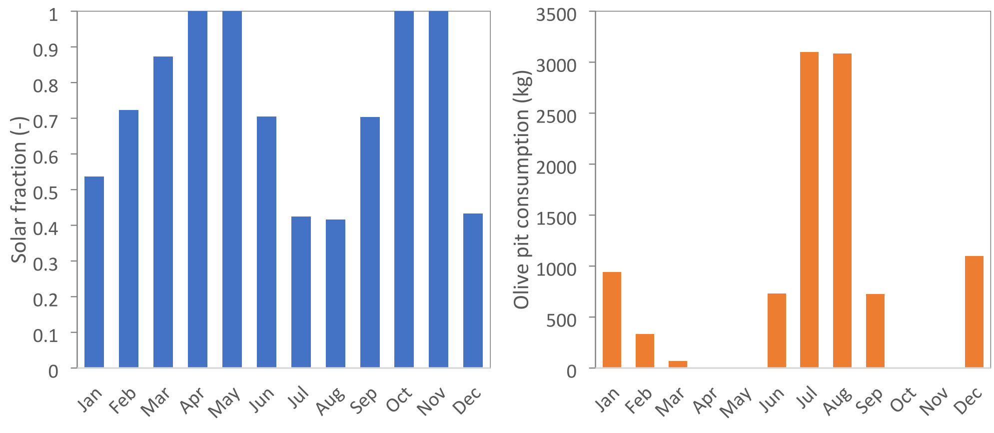

(a)

Fig. 13. Monthly solar fraction of the proposed system (a), and monthly olive pits consumption (b).

$$SF = \frac{Q_{SS}}{Q_{GH}} \tag{15}$$

As can be observed, 100 % of the solar fraction is reached during the spring and autumn, as expected from the previous results. Moreover, 70 % of the solar fraction is gotten for eight months, except for July and August in summer, when only 42 % and 41 % of the solar fraction is reached despite the higher solar production during these months, and January and December when only 54 % and 43 % of the solar fraction is reached.

In addition, Fig. 13 (b) shows the monthly olive pits consumption of the system. As expected, July and August are the months with the highest olive pits consumption, with more than 3,000 kg for these months. For the coolest months of the year with lower solar radiation, January and December, the olive pit consumption is about 1,000 kg.

In Table 7, the annual results of the heating and cooling system coupled to the greenhouse are summarized. It can be observed that the thermal production of the solar system is slightly higher than the boiler consumption, leading to an annual solar fraction of about 54.9 %. The annual olive pit consumption is 10068 kg, which means that (assuming a cost of 0.30 €·kg_{pits}^{-1}) the annual cost of the fuel is about 3,020 €.

4. Conclusions and future works

A thermal model of a greenhouse has been developed on the TRNBuild tool. This model is validated with real data taken from a greenhouse located in the southeast of Spain. When comparing the results obtained with the dynamic model with real measurements, minor discrepancies are found for a week in April. The validated model allows us to easily couple it with heating and cooling systems to obtain the seasonal performance of the system, and indoor air conditions and to evaluate control strategies.

The validated model was used to obtain the annual heating and cooling demands of the greenhouse for tomato crops. In this sense, the annual heating demand is 26.37 kW·h·m^{-2} and the annual cooling demand is 61.97 kW·h·m^{-2}. This represents 29.9 % and 70.1 % of the total thermal energy demand, respectively. Regarding the peak loads, the heating peak load is 142.8 W·m^{-2} and the cooling peak load is 177.0 W·m^{-2}.

Table 7
Annual results of the heating and cooling system for the greenhouse.

Annual result	Value
Heating demand (kW·h)	29,510
Cooling demand (kW·h)	69,407
Solar thermal production (kW·h)	63,071
Boiler consumption (kW·h)	60,127
Olive pit consumption (kg)	10,068
Solar Fraction (%)	54.92
Solar collectors' seasonal efficiency (%)	34.03
Absorption chiller seasonal COP (-)	0.624

A heating and cooling system based on evacuated-tube solar thermal collectors, a biomass boiler, and an air-cooled absorption chiller with ammonia/lithium nitrate as a working mixture is proposed to control the environmental conditions of a greenhouse located in the southeast of Spain. Both, the proposed heating and cooling system model and the greenhouse model have been coupled in TRNSYS to study the system operation and to obtain the seasonal performance of the proposed system. The specification of the main components (absorption chiller capacity, solar collector technology, and absorbance area, biomass boiler thermal capacity, water tank volume…) as well as the operational temperatures for winter and summer conditions are proposed.

When analyzing the system operation, five different operational modes are required for both, winter, and summer. It is also figured out that the water tank is especially important in winter months as the solar energy available and the heating demand are completely disengaged.

Moreover, under these climatic conditions, a passive greenhouse must stop crop production from the middle of May until the beginning of October, as the indoor air temperature is too high. However, with the proposed heating and cooling system, indoor air conditions are optimal for the whole year, leading to higher crop productivity.

With this system, it is found that, during the spring and autumn months, the solar collector produced more heating than required by the greenhouse. Therefore, the excess thermal energy could be used for other purposes or finer control of the greenhouse indoor conditions, which might lead to higher crop productivity during these months. On the other hand, 61.4 % of boiler consumption only takes place during July and August, although solar thermal production is the highest during these two months.

The annual solar fraction reached by the system is 54.9 %. A solar fraction of 100 % is reached during 4 months of the year. However, during July and August the solar fraction reached is only 42 % and 41 % respectively. This leads to taking into consideration if it is economically feasible to use the greenhouse during these two months when the biomass consumption is too high.

As future works, it is expected to integrate crop productivity models with the developed model presented in this study. This integration will help us to obtain the enhancement in terms of tomato production reached with this proposed system. Moreover, results gotten from this study and the integrated productivity model will be used for a detailed economic analysis of the proposed heating and cooling system.

Declaration of Competing Interest

The authors declare the following financial interests/personal relationships which may be considered as potential competing interests: Pablo Fernandez- del Olmo reports financial support was provided by European Regional Development Fund.

Data availability

Data will be made available on request.

Acknowledgments

This work has been co-financed at 80 % by the European Regional Development Fund (ERDF), Operational Program of Andalusia 2014-2020, collaborating with IFAPA through Project AVA.AVA2019.039 “New technologies in protected horticulture: Efficiency in the use of natural resources and energy from renewable sources”. Also, the research work presented in this paper is the outcome of a project funded by Diputació de Tarragona under the collaboration framework agreement between the Diputació de Tarragona and the Universitat Rovira i Virgili for the period 2020–2023 with the reference number 2022/#.

References

[1] U. Nations, “Transforming our World: The 2030 Agenda for Sustainable Development.” 2015. doi: 10.1201/b20466-7.
[2] G.J. Hochmuth, R.C. Hochmuth, Production of Greenhouse Tomatoes, Florida Greenhouse Vegetable Production Handbook 3 (2018) 1–18.
[3] G. Nikolaou, D. Neocleous, N. Katsoulas, C. Kittas, Effects of cooling systems on greenhouse microclimate and cucumber growth under mediterranean climatic conditions, Agronomy 9 (6) (2019) pp, https://doi.org/10.3390/agronomy9060300.
[4] I. Tsafaras, J.B. Campen, C. Stanghellini, H.F. de Zwart, W. Voogt, K. Scheffers, A. Al Harbi, K. Al Assaf, Intelligent greenhouse design decreases water use for evaporative cooling in arid regions, Agricultural Water Management, vol. 250, no. June 2020, p. 106807, 2021, doi: 10.1016/j.agwat.2021.106807.
[5] M. Fuchs, E. Dayan, E. Presnov, Evaporative cooling of a ventilated greenhouse rose crop, Agric. For. Meteorol. 138 (1–4) (2006) 203–215, https://doi.org/10.1016/j.agrformet.2006.05.002.
[6] C.K.N.C. Sabeh, G.A. Giacomelli, Water Use in a Greenhouse in a Semi-Arid Climate, Trans. ASABE 54 (3) (2011), https://doi.org/10.13031/2013.37098.
[7] G. Zaragoza, M. Buchholz, P. Jochum, J. Pérez-Parra, Watergy project: Towards a rational use of water in greenhouse agriculture and sustainable architecture, Desalination 211 (1–3) (2007) 296–303, https://doi.org/10.1016/j.desal.2006.03.599.
[8] Wageningen University, “Saudi Arabia: Research greenhouse shows water-saving possibilities,” January 30, 2018. https://www.hortidaily.com/article/40832/Saudi-Arabia-Research-greenhouse-shows-water-saving-possibilities/ (accessed Feb. 10, 2022).
[9] D.S. Ayou, G. Zaragoza, A. Coronas, Small-scale renewable polygeneration system for off-grid applications: Desalination, power generation and space cooling, Appl. Therm. Eng., vol. 182, no. October 2020, p. 116112, 2021, doi: 10.1016/j.applthermaleng.2020.116112.
[10] D.S. Ayou, A. Coronas, New developments and progress in absorption chillers for solar cooling applications, Appl. Sci. 10 (12) (2020) pp, https://doi.org/10.3390/app10124073.
[11] C.A. Campiottia, G. Morosinottob, G. Puglisia, E. Schettinic, G. Vox, Performance evaluation of a solar cooling plant applied for greenhouse thermal control, Agric. Agric. Sci. Procedia 8 (2016) 664–669, https://doi.org/10.1016/j.aaspro.2016.02.076.
[12] M.S. Ahamed, H. Guo, K. Tanino, Modeling heating demands in a Chinese-style solar greenhouse using the transient building energy simulation model TRNSYS, J. Build. Eng., vol. 29, no. December 2019, p. 101114, 2020, doi: 10.1016/j.jobe.2019.101114.
[13] A. Vadiee, V. Martin, Energy analysis and thermoeconomic assessment of the closed greenhouse - The largest commercial solar building, Appl. Energy 102 (2013) 1256–1266, https://doi.org/10.1016/j.apenergy.2012.06.051.
[14] L. Zhang, P. Xu, J. Mao, X. Tang, Z. Li, J. Shi, A low cost seasonal solar soil heat storage system for greenhouse heating: Design and pilot study, Appl. Energy 156 (2015) 213–222, https://doi.org/10.1016/j.apenergy.2015.07.036.
[15] S. Agrebi, R. Chargui, B. Tashtoush, A.A. Guizani, Comparative performance analysis of a solar assisted heat pump for greenhouse heating in Tunisia, Int. J. Refrig 131 (2021) 547–558, https://doi.org/10.1016/j.ijrefrig.2021.06.004.
[16] J.A. Sánchez-Molina, J.V. Reinoso, F.G. Acién, F. Rodríguez, J.C. López, Development of a biomass-based system for nocturnal temperature and diurnal CO2 concentration control in greenhouses, Biomass Bioenergy 67 (2014) 60–71, https://doi.org/10.1016/j.biombioe.2014.04.015.
[17] M.J. Sánchez-González, M.C. Sánchez-Guerrero, E. Medrano, M.E. Porras, E. J. Baeza, P. Lorenzo, Carbon dioxide enrichment: A technique to mitigate the negative effects of salinity on the productivity of high value tomatoes, Span. J. Agric. Res. 14 (2) (2016) pp, https://doi.org/10.5424/sjar/2016142-8392.
[18] M. Kummert, “Multizone Building modeling with Type56 and TRNBuild,” in TRNSYS 16 a TRaNsient SYstem Simulation program, vol. 6, 2007.
[19] D. Valera, L. Belmonte, F. Molina-Aiz, A. López, Los invernaderos de Almería Análisis de su tecnología y rentabilidad, 2014. Editor: Cajamar Caja Rural.
[20] C. Stanghellini, T. De Jong, A model of humidity and its applications in a greenhouse, Agric. For. Meteorol. 76 (1995) 129–148.
[21] T. Kasuda, P.R. Archenbach, Earth Temperature and Thermal Diffusivity at Selected Stations in the United States, ASHRAE Trans. 71 (Part 1) (1965).
[22] P.J.M. Van Beveren, J. Bontsema, G. Van Straten, E.J. Van Henten, Minimal heating and cooling in a modern rose greenhouse, Appl. Energy 137 (2015) 97–109, https://doi.org/10.1016/j.apenergy.2014.09.083.
[23] A. Ruiz-García, I.L. López-Cruz, R. Arteaga-Ramírez, J.A. Ramírez-Arias, Tasas de ventilación natural de un invernadero del centro de México estimadas mediante balance de energía, Agrociencia 49 (1) (2015) 87–100.
[24] H. M. Hellmann, C. Schweigler, F. Ziegler, A simple method for modelling the operating characteristics of absorption chillers, in Proceedings of Thermodynamics Heat and Mass Transfers of Refrigeration Machines and Heat Pumps Seminar EUROTHERM N° 59, 1998, pp. 219–226.
[25] M. Zamora-García, Optimización industrial y estrategia de control de una enfriadora de absorción de amoniaco / nitrato de litio con disipación por aire, Universitat Rovira i Virgili, 2014. Doctoral Thesis.
[26] S.P. Forschung, Collector Test No. C250: SK-6, 1999.
[27] EnergyPlus, Weather Data by Location, 2020. https://energyplus.net/weather-location/europe_wmo_region_6/ESP//ESP_Almeria.084870_SWEC (accessed Feb. 11, 2002).
[28] A. Van't Ooster, W. Van Ieperen, P. Kalaitzoglou, Model study on applicability of a semi closed greenhouse concept in Almeria: Effects on greenhouse climate, crop yield and resource use efficiency, Acta Horticulturae, vol. 927, pp. 51–58, 2012, doi: 10.17660/ActaHortic.2012.927.4.